ELSEVIER

Thin Solid Films 297 (1997) 237–240

thin solid films

Dielectric filters made of PS: advanced performance by oxidation and new layer structures

M.G. Berger [a], R. Arens-Fischer [a], M. Thönissen [a], M. Krüger [a], S. Billat [a], H. Lüth [a], S. Hilbrich [b], W. Theiß [b], P. Grosse [b]

[a] *Institut für Schicht- und Ionentechnik (ISI), KFA Jülich, D-52425, Jülich, Germany*
[b] *Physikalisches Institut der RWTH Aachen, D-52056, Aachen, Germany*

Abstract

For the formation of PS dielectric filters a detailed calibration of the etch rates and refractive indices is required. The effective dielectric function of PS was determined for different substrate doping levels as a function of the anodization current density by fitting reflectance spectra. Based on these results a number of different dielectric filters were realized. For device applications a thermal oxidation step is necessary to reduce aging effects which occur as a result of the native oxidation of PS. In addition, thermal oxidation results in a qualitatively improve filter performance due to a reduced absorption in the PS layers. Therefore the dielectric functions of PS oxidized in dry O_2 at temperatures up to 950 °C were determined. A continuous variation of the porosity and hence the refractive index with depth was used to realize so-called rugate filters. This type of interference filter allows the design of structures with more complex reflectance or transmittance characteristics than structures consisting of discrete single layers. © 1997 Elsevier Science S.A.

Keywords: Thermal oxidation; PS layers; Oxidation

1. Introduction

Porous silicon multilayer structures have been intensively studied by several research groups [1–7]. The majority of these studies were concerned with the optical properties of controlled layer stacks which can be used as interference filters [8]. Although filters are the most obvious application of PS multilayers, waveguiding properties of PS layer stacks have also been studied [9].

Within this paper we will focus on the properties of PS multilayers used as interference filters. Possible applications of such filters were recently demonstrated and include the fabrication of low cost infrared sensors which serve as chemometric detectors [10] and the combination of PS interference filters for the visible spectral range with conventional silicon photodiodes [11]. For both kinds of applications well-defined reflectance/transmittance characteristics are required. In addition, for color-sensitive silicon photodiodes a high-quality filter performance in the blue/violet part of the visible spectral range must be achieved.

In this paper it will be shown that the latter can be fulfilled by a thermal oxidation of PS multilayers, resulting in a porous silicon-oxide multilayer. To obtain filters with improved and/or more complex reflectance/transmittance characteristics, rugate filters are promising candidates. These kinds of filters are characterized by a continuous change of the refractive index with depth and are well known in optics to allow the realization of fascinating filter properties [12,13]. We will demonstrate that PS is very well suited for the formation of rugate filters, which clearly show improved filter characteristics as compared to conventional PS multilayer stacks.

2. Experimental

PS layers were formed by the anodization of Czochralski-grown boron doped silicon (100) wafers. PS layers on substrates with resistivities of 10 mΩ cm (p^+) and 200 mΩ cm (p) were investigated. For the p-doped substrates a metal contact was evaporated on the backside of the wafer to allow a homogeneous current flow. Immediately before anodization the substrates were cleaned in propanol in an ultrasonic bath and rinsed in deionized water. Anodization was performed under standard galvanostatic conditions using a mixture of H_2O:HF:C_2H_5OH = 1:1:2. The anodization current was supplied by a Keithley 238 high-precision constant current source which is controlled by a computer to allow the formation of PS multilayers. To prevent the photogeneration of carriers, the anodization is performed in the dark. After formation the samples are rinsed with pure ethanol and dried with nitrogen gas.

Reflectance spectra of the samples were taken with a Perkin Elmer λ2 photospectrometer in the range of 9000–

PII S0040-6090(96)09361-3

50 000 cm^{-1} (1111–200 nm). The reflectance was measured under an incidence angle of 8° using s-polarized light. From the reflectance spectra of single porous layers the effective dielectric function of PS was deduced by a fitting procedure (for details see Ref. [14]). The etch rate as a function of the anodization current density was determined by a thickness measurement of the PS layer using a scanning electron microscope (SEM). Thermal oxidation of the PS was performed at 950 °C for 5 min.

3. Results and discussion

For the formation of interference filters the effective refractive index and the etch rate must be known as a function of the anodization current density. In addition, for filters with different filter wavelengths the rather strong dispersion of the refractive index in the visible spectral range must be considered.

To minimize any depth gradients in the porous layer [15] the etch rate and effective dielectric function was obtained from samples formed with different anodization current densities each having a layer thickness of only about 1 μm. The results are shown in Fig. 1. For simplicity the effective refractive index is shown for a wavenumber of 12 000 cm^{-1} (833 nm) only, while data were obtained with high accuracy in the range of 9000–25 000 cm^{-1} (1111–400 nm). For both substrates the etch rate can be well described as $r \propto j/(P(j)\cdot v(j))$, assuming a linear dependence of the porosity $P(j)$ and the valence $v(j)$ on the current density j.

The most obvious difference between the p- and p^+-substrates is the much broader range of refractive indices which can be obtained in the latter case. The reason therefore is the broader range of porosities which can be achieved for p^+-substrates (20–90%) as compared to only 65–85% for p-substrates. Again, for both substrate doping levels the refractive index has been fitted as a function of the wavenumber and the anodization current density to simplify the calculation of etch parameters for interference filter formation.

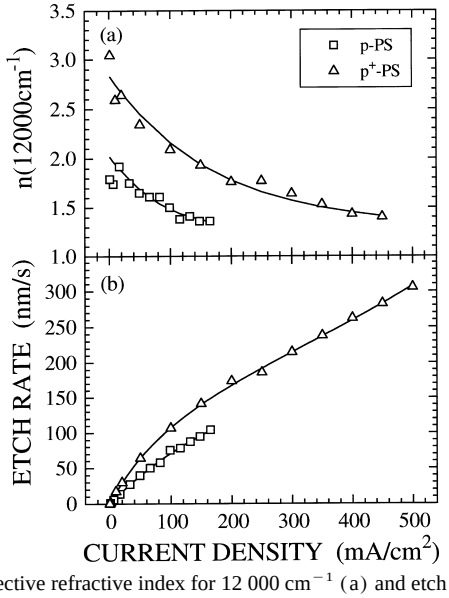

Fig. 1. Effective refractive index for 12 000 cm^{-1} (a) and etch rate (b) as a function of the anodization current density for two different substrate doping levels.

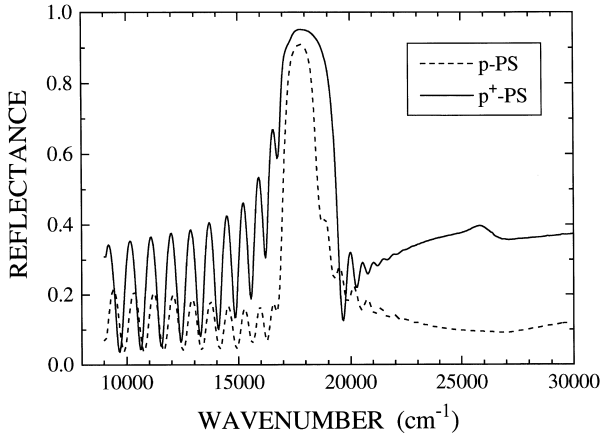

Fig. 2. Reflectance spectra of Bragg reflectors $[HL]^{20}$ formed on p- and p^+-doped substrate. The current densities used for the formation of the H/L-layer were 30/120 mA cm^{-2} for the p-doped substrate and 20/400 mA cm^{-2} for the p^+-doped substrate.

For the formation of interference filters in the visible spectral range the consequences of using different substrate doping levels must be considered. The discussion will be restricted to Bragg reflectors which consist of a periodical stack of quarterwave layers with alternating high (H) and low (L) refractive index. In optics such a layer stack is usually denoted as $[HL]^n$, where n equals the number of periods of the HL layers. The reflectance spectrum of a Bragg reflector is characterized by a high reflectance peak around the design wavelength whereas the reflectance for other wavelengths is low (see Fig. 2). For a given number of periods the height and width of the reflectance peak increases with increasing index ratio H/L. This is demonstrated in Fig. 2 where a Bragg reflector $[HL]^{20}$ has been formed using p- and p^+-substrate. For the p^+-doped substrate an index ratio of 1.8 was used, whereas for the p-doped substrate only an index ratio of 1.18 could be obtained. However, the disadvantage of a low index ratio can be compensated by a higher number of periods. Hence, increasing the overall PS layer thickness causes a depth inhomogeneity in the layer stack which is much higher for the p^+-doped substrate due to the high current density required for the formation of the L-layers (see Ref. [15]). This depth inhomogeneity seriously degrades the filter performance. Another important fact which favors the use of p-doped substrates is the microporous structure as opposed to the mesoporous structure of PS formed on the p^+-doped substrates. The difference in the microstructure has two consequences. Firstly, the interface sharpness between layers of different porosity was found to depend on the microstructure, resulting in values for the thickness of the interface gradient of about 10 nm for p-doped substrates as compared to about 20 nm for p^+-doped substrates [16]. Secondly, the absorption of light in the visible spectral range is known to be higher for mesoporous PS [17]. Although the absorption of light is lower for microporous PS formed on p-doped substrates due

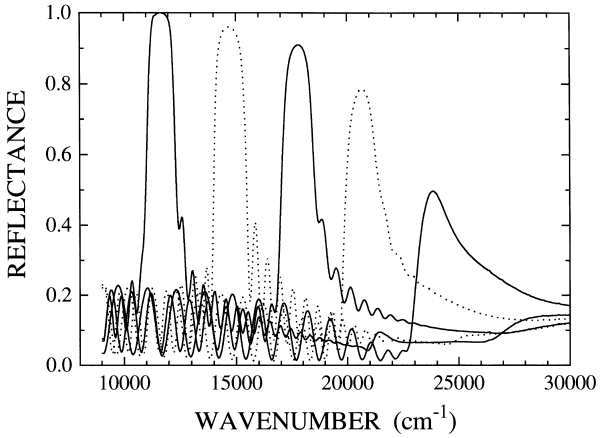

Fig. 3. Reflectance spectra of different Bragg reflectors $[HL]^{20}$ exhibiting reflectance peaks over the whole visible spectral range. The samples were formed on p-doped substrate using current densities of 30/120 mA cm^{-2} for the H/L layer, respectively. The decrease of the peak maximum is due to light absorption in the filter structure.

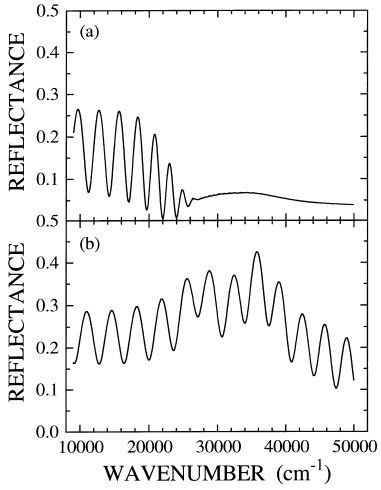

Fig. 4. Reflectance spectra of a single porous layer formed on p-doped substrate (thickness 1 μm, anodization current density 120 mA cm^{-2}) (a) before and (b) after thermal oxidation (950 °C for 5 min).

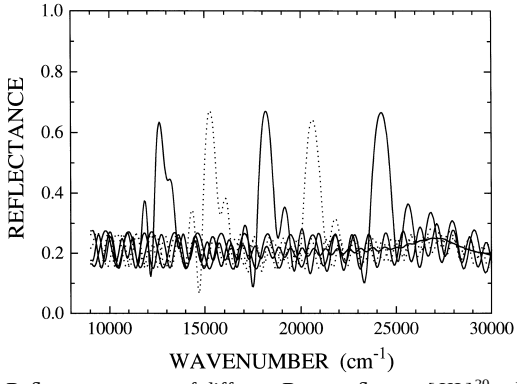

Fig. 5. Reflectance spectra of different Bragg reflectors $[HL]^{20}$ exhibiting reflectance peaks over the whole visible spectral range. The samples were formed on p-doped substrate using current densities of 80/120 mA cm^{-2} for the H/L layer, respectively. After formation the samples were thermally oxidized in dry O_2 at 950 °C for 5 min. The height of the reflectance peak does not decrease with increasing wavenumber.

to the higher band gap of this material, it is still strong enough to drastically decrease the height of the reflectance peak for Bragg reflectors in the blue/violet spectral range. This is shown in Fig. 3 for different Bragg reflectors $[HL]^{20}$, formed on p-doped substrate, exhibiting reflectance peaks throughout the whole visible spectral range (12 000–24 000 cm^{-1}). While the filter for 12 000 cm^{-1} reaches a maximum reflectance of about 100% the height of the maximum shows a continuous decrease with increasing wavenumber.

To improve the filter performance in the blue/violet spectral range, the absorption in the PS must be decreased. This can be achieved by a complete oxidation of the porous silicon, resulting in a transparent porous siliconoxide. From FIPOS technology [18] it is known that a complete oxidation of PS causes a volume increase of the silicon skeleton by about a factor of two. Therefore the porosity of both the *H*- and *L*-layers must be well above 50% before oxidation, in order to prevent a closing of the pores and to allow a complete oxidation of multilayers over the whole layer thickness.

PS single layers of 1 μm thickness have been thermally oxidized in dry O_2 for 5 min at different temperatures. For an oxidation temperature of 950 °C the Fabry–Perot interferences which are visible for wavenumbers lower than 26 000 cm^{-1} only for the unoxidized sample due to the decreasing light penetration depth [see Fig. 4(a)], can be observed over the whole measured spectral range [Fig. 4(b)]. This indicates a more or less complete oxidation of the silicon skeleton for these oxidation parameters.

Again, the effective refractive index of single layer samples formed with different anodization current densities has been determined after a period of 5 min thermal oxidation at 950 °C, and used as input for the fabrication of porous silicon oxide Bragg reflectors. The results are shown in Fig. 5. The layer structure of these filters was $[HL]^{20}$ as in the case of Fig. 3. However, due to the lower refractive index of SiO_2 as compared to silicon, the index ratio H/L decreases, e.g. from 1.18 to 1.13 for the oxidized Bragg reflector for 12 000 cm^{-1} as compared to the unoxidized Bragg reflector. This causes a decrease and a narrowing of the reflectance peak which can be clearly observed. In contrast to the unoxidized filters, the height of the reflectance peak does not decrease when increasing the filter wavenumber, but maintains a peak reflectance value about 65% even for the filter at 24 000 cm^{-1} (50% for the unoxidized filter). For further enhancement of the peak reflectance value an increase in the number of periods would be required, as already mentioned above. However, for increasing overall layer thickness the depth inhomogeneity of PS becomes important [15]. These inhomogeneities cause a depth-dependent shift of the reflectance peak, which in the case of very narrow reflectance peaks causes the peak to smear out instead of the desired increase of the reflectance maximum. Therefore, it is planned to improve the in depth homogeneity of the layers using the results obtained in Refs [15,19].

A different ansatz for improving the filter characteristics is the use of rugate filter structures. Put simply, in rugate filters the discrete layer structure is substituted by a continuous, mostly sinusoidal change of the refractive index with

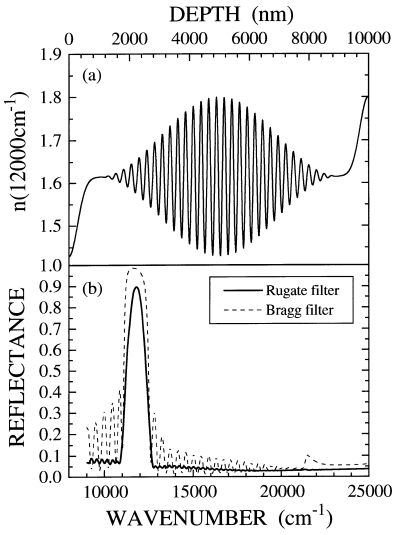

Fig. 6. Depth profile of the refractive index (a) and reflectance spectrum (b) of a rugate filter formed on p-doped substrate. For comparison the reflectance spectrum of a Bragg reflector $[LH]^{24}$ is shown. In contrast to the Bragg reflector the rugate filter is characterized by the absence of sidelobes around the reflectance peak.

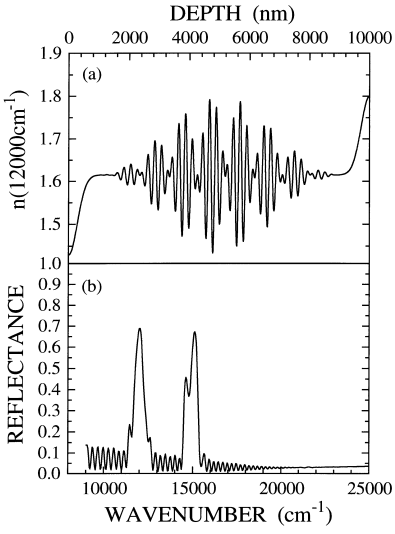

Fig. 7. Depth profile of the refractive index (a) and reflectance spectrum (b) of a rugate filter formed on p-doped substrate. The index profile is a superposition of two sine functions with different periods resulting in two reflectance peaks at different wavelengths.

depth. For a detailed discussion of rugate filters see, for example, Refs [12,13]. Due to the dependence of the effective refractive index on the anodization current density (Fig. 1) PS is very well suited for the fabrication of rugate filters. From theoretical calculations [13] an index profile as shown in Fig. 6(a) is expected to result in a very ''clean'' reflectance spectrum without strong sidelobes. Using the calibration curves from Fig. 1 such a filter has been formed on p-doped substrate. The resulting reflectance spectrum is shown in Fig. 6(b). For comparison, the reflectance spectrum for a standard Bragg reflector $[LH]^{24}$ is also shown. In contrast to the standard Bragg reflector the reflectance spectrum of the rugate filter is characterized by the almost complete absence of sidelobes over the whole spectral range and a very low reflectance value ($<10\%$). A minor drawback is the reduction of the peak reflectance of the rugate filter compared to the Bragg reflector.

Besides reducing the sidelobes, rugate filters allow a greater freedom in filter design. This is demonstrated in Fig. 7, which shows the index profile and reflectance spectrum of a filter exhibiting reflectance peaks at two different wavelengths. The index profile of this filter is a superposition of two sine functions with different periods. This technique can be used to obtain almost any desired reflectance spectrum.

4. Conclusion

To conclude, we have shown that thermal oxidation of PS multilayers can be used to completely oxidize the silicon skeleton, resulting in a porous siliconoxide interference filter. Due to their low absorption in the short wavelength range of the visible spectrum these filters exhibit a better performance as compared to conventional PS interference filters. In addition, for the first time porous silicon rugate filters including matching layers have been formed. Rugate filters allow a suppression of unwanted sidelobes in the reflectance spectra and offer a large degree of freedom in filter design.

References

[1] M.G. Berger, C. Dieker, M. Thönissen, L. Vescan, H. Lüth, H. Münder, W. Theiß, M. Wernke and P. Grosse, *J. Phys. D: Appl. Phys.*, *27* (1994) 1333.
[2] M.G. Berger, R. Arens-Fischer, S. Frohnhoff, C. Dieker, K. Winz, H. Münder, H. Lüth, M. Arntzen and W. Theiß, *Mater. Res. Soc. Symp. Proc.*, *358* (1995) 327.
[3] G. Vincent, *Appl. Phys. Lett.*, *64* (1994) 2367.
[4] D. Buttard, D. Bellet and T. Baumbach, *Thin Solid Films*, *276* (1996) 69.
[5] C. Mazzoleni and L. Pavesi, *Appl. Phys. Lett.*, *67* (1995) 2983.
[6] Xing-Long Wu, *Appl. Phys. Lett.*, *68* (1996) 611.
[7] M. Araki, *Jap. J. Appl. Phys. 35*, 2B, (1996) 1041.
[8] M.G. Berger, S. Frohnhoff, R. Arens-Fischer, M. Thönissen, C. Dieker, H. Münder, H. Lüth and W. Theiß, Optical interference coatings, in F. Abeles (ed.), *Proc. SPIE 2253*, 1994, p. 865.
[9] A. Loni, R.J. Bozeat, M. Krueger, M.G. Berger, R. Arens-Fischer, M. Thönissen, H.F. Arrand and T.M. Benson, *Proc. IEE Colloquium, Microengineering Applications in Optoelectronics, 27 February, 1996, London*, Digest no. 96/39.
[10] S. Hilbrich, W. Theiß, R. Arens-Fischer, M.G. Berger, M. Krüger and M. Thönissen, *Thin Solid Films, 297*, (1997).
[11] M. Krüger, M. Marso, M.G. Berger, M. Thönissen, S. Billat, R. Loo, W. Reetz, H. Lüth, S. Hilbrich, R. Arens-Fischer and P. Grosse, *Thin Solid Films, 297* (1997).
[12] B.G. Bovard, *Appl. Opt., 32*, 28 (1993) 5427.
[13] W.H. Southwell, *Appl. Opt., 28*, 23 (1989) 5091.
[14] W. Theiß, R. Arens-Fischer, M. Amtzen, M.G, Berger, S. Frohnhoff, S. Hilbrich and M. Wernke, *Mater. Res. Soc. Symp. Proc., 358* (1995) 435.
[15] M. Thönissen, M.G. Berger, S. Billat, R. Arens-Fischer, M. Krüger, H. Lüth, W. Theiß, S. Hilbrich, P. Grosse, G. Lerondel and U. Frotscher, *Thin Solid Films, 297* (1997).
[16] M.G. Berger, *Ph.D. Thesis*: Poröses Silicium für die Mikrooptik: Herstellung, Mikrostruktur und optische Eigenschaften von Einzelschichten und Schichtsystemen, RWTH Aachen, 1996.
[17] I. Sagnes, *Appl. Phys. Lett., 62*, 10 (1993) 1155.
[18] G. Bomchil et al., *Microelectron. Engng, 8* (1988) 293.
[19] S. Billat, M. Thönissen, R. Arens-Fischer, M.G. Berger, M. Krüger and H. Lüth, *Thin Solid Films, 297* (1997).